Phys. Status Solidi C **12**, No. 4–5, 376–380 (2015) / **DOI** 10.1002/pssc.201400176

physica status solidi c
www.pss-c.com
current topics in solid state physics

Blue to true green LEDs with semipolar quantum wells based on GaN nanostripes

Robert A. R. Leute[*,1], Junjun Wang[1], Tobias Meisch[1], Joachim Biskupek[2], Ute Kaiser[2], and Ferdinand Scholz[1]

[1] Institute of Optoelectronics, Ulm University, Ulm, Germany
[2] Central Facility of Electron Microscopy, Ulm University, Ulm, Germany

Received 14 July 2014, revised 4 December 2014, accepted 20 January 2015
Published online 16 March 2015

Keywords MOVPE, semipolar, GaN, LED, green gap

[*] Corresponding author: e-mail robert.leute@uni-ulm.de

Recent advances of the performance of GaN based devices with semipolar quantum wells have been realized homoepitaxially on pseudo bulk substrates which are typically small in size and high in cost. These limitations fuel the search for cheap and large area alternatives. Heteroepitaxial growth on sapphire substrates is well established with excellent results for polar GaN structures - the growth of semipolar gallium nitride on sapphire, however, presents unique challenges. In order to profit from our expertise in c-plane samples, our semipolar gallium nitride growth experiments are based on growth in c-direction. Using selective area epitaxy (SAE) on c-oriented templates, we can grow 3D structures with semipolar side facets. These structures are typically several µm in size which constitutes further challenges for device processing. Reducing the size of the structures to a sub-µm scale, we are able to bury our semipolar QWs within planar layers resulting in flat samples with c-plane surfaces. In this contribution, we present our results concerning the structural quality and spectral properties of quantum wells emitting in the blue and green spectral range as well as light emitting diodes.

1 Introduction Semipolar GaN crystal planes still attract strong research interest for efficient green light emitters [1,2]. Best results have been achieved based on free-standing GaN templates and homoepitaxial approaches [3–5]. These semipolar GaN quasi-substrates are commercially available but costly and small in size. Huge progress has been made [6] but the comparison to c-plane oriented pseudo-bulk [7] is still highly unfavorable. Consequently, heteroepitaxy of semipolar GaN based on cheap sapphire substrates remains important [8]. In the following, we present results on heteroepitaxial growth of semipolar GaN on sapphire. In order to profit from the high crystal quality achieved for c-oriented GaN on sapphire [9], we base our approach on the selective growth of 3D structures with semipolar surfaces. Thus, it can be realized on cheap and large substrates. High crystal quality has already been achieved [10] and LEDs with semipolar QWs based on m sized 3D structures have been reported [11–15]. Yet, these 3D topologies require specially adapted device processing. Within this manuscript, we present our current results, addressing the issues of large area manufacture and flat sample surfaces despite 3D growth.

2 Selective growth for semipolar quantum wells

Selective area epitaxy (SAE) has been used for decades [16] in order to improve crystalline quality. The c-oriented surface of a GaN template is covered with a dielectric mask. Depending on the patterning of the growth mask and the growth parameters, we observe the formation of pyramids, inverse pyramids or stripes with triangular cross-section. These inclined surfaces are the naturally stable crystal facets $\{10\bar{1}1\}$ and $\{11\bar{2}2\}$. While vertical (non-

polar) side facets can be realized, too, they are not focus of this work. A review of 3D growth can be found in [10]. For direct electrical operation of LEDs, flat sample surfaces are far more convenient and compatible with conventional processing. Reducing the size of the 3D structures allows us to use them exclusively within the active region of our aspired devices. This miniaturization allows subsequent planarization (see Fig. 1). All dimensions must be restricted to a few hundred nanometers, beyond the limitations of conventional optical lithography. Previously, we have reported on nanostructuring for selective area epitaxy based on laser interference lithography (LIL) for LED [17] and photonic crystal applications [18]. However, the LIL samples still suffered from mask irregularities and the structured area was limited to some cm^2, which is why an alternative structuring method was used as described in the following.

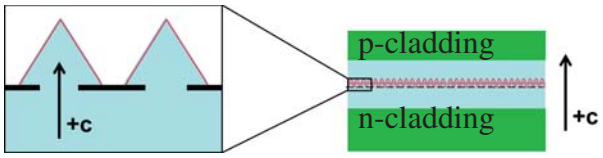

Figure 1 Reduction of size of 3D GaN will allow embedding of semipolar QWs within conventional c-oriented layers.

2.1 Experimental All epitaxial growth takes place inside an Aixtron-200/4RF-S HT MOVPE reactor with standard precursors TMAl, TMGa, TMIn and high purity ammonia. Silane and Cp_2Mg are used for n- and p-doping, respectively; Pd diffused hydrogen and high purity nitrogen are used as carrier gases.First, c-oriented GaN/AlGaN templates of about 3.5 µm thickness are grown on c-plane sapphire with conventional growth conditions. An oxygen doped AlN nucleation layer as well as an in-situ deposited SiN interlayer are employed for defect reduction [19]. The top 1.8 µm are silicon-doped to achieve a nominal doping level of $3.5 \times 10^{18} cm^{-3}$. The templates include a 0.4 µm thick $Al_{0.1}Ga_{0.9}N$ as bottom waveguide cladding and are capped with 30 nm GaN. Afterwards, 30 nm SiN_x is deposited by PECVD as growth mask. Upon this dielectric mask, a very thin (below 100 nm) layer of resist is structured by nanoimprint lithography. Dry etching with SF_6, results in stripes aligned parallel to the a-direction of GaN with a period of 250 nm over the full 2-inch wafer. Afterwards, any remaining resist is removed by an O_2-plasma treatment and the samples are cleaned with a mixture of H_2O_2 and H_2SO_4 and an aqueous KOH solution, before being reloaded into the MOVPE reactor. GaN stripes with a triangular cross-section and $\{10\bar{1}1\}$ side facets are grown at 950 °C for 110 s with a V/III ratio of 260. An InGaN pre-well of 50 nm thickness with 5% In is deposited on top of the stripes, in order to reduce the strain gradient and increase the confinement. A single InGaN quantum well with GaN barriers is grown at 740 °C to 770 °C to achieve an emission wavelength of 410 nm to 530 nm. The QW is covered with a 3D undoped spacer, then the stripes are buried with a Mg-doped layer grown at 1080 °C for blue QWs and at 960 °C for green QWs with a V/III ratio of 1080, resulting in a planar surface. At this point, the structure does not include an electron blocking layer common to c-plane LEDs. The full process is depicted in Fig. 2. The fully planarized LED structures were investigated by transmission electron microscopy (TEM) after subsequent preparation of cross section TEM samples. Conventional bright- and dark-field TEM experiments for analysis of the crystal structure of the LEDs were carried out using a Philips CM20 operating at 200 kV. Scanning transmission electron microscopy (STEM) was carried out using a FEI Titan 80-300 operating at 300 kV equipped with a high angle annular dark-field (HAADF) detector. STEM imaging was applied to investigate the QWs in more details by exploiting the Z-contrast mode of the HAADF detector. For electrical characterization, the samples were annealed in an ambient atmosphere at 750 °C for 60 s to activate the Mg-acceptors. Indium contacts were evaporated onto the p-side of the LED. The contacts had diameters ranging from 70 µm to 140 µm and were 1 µm thick. Measurements were taken on-wafer without further light-extraction measures inside an integrating sphere and P-I as well as I-V curves were recorded. Furthermore the emitted light was analyzed with a monochromator with a 300/mm grating and an electrically cooled CCD camera.

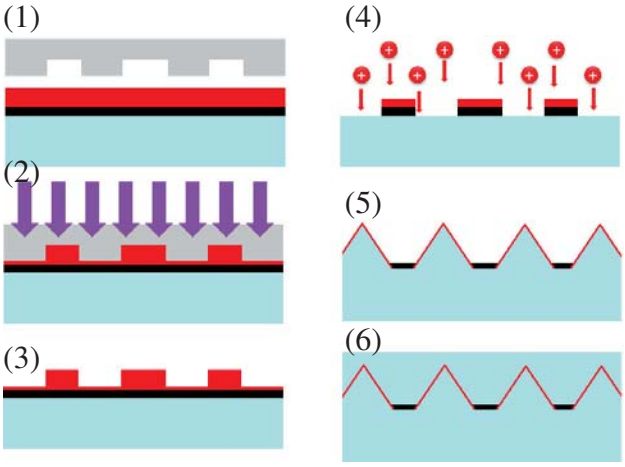

Figure 2 Fabrication process for nanostripe LEDs. A PMMA stamp (1) is pressed into the resist, after UV curing (2) the resist is polymerized and the pattern transfered (3). Dry etching in a fluorine plasma (4) transfers the pattern into the dielectric growth mask. Selective epitaxy (5) results in stripes with semipolar side facets on which the QWs are deposited. Finally they are embedded, resulting in a planar surface (6).

3 Results We achieved homogeneous growth of submicrometer sized stripes aligned along the GaN a-direction over the complete sample area enabling subsequent embedding. Mg doping enhances the lateral growth [20] and facilitates the planarization of the device. Yet, the stability of

the $\{10\bar{1}1\}$ facets [16] requires relatively long overgrowth times (equivalent to 180 nm layer thickness) compared to typical c-plane LED p-type layers.

3.1 Structural analysis Figure 3 shows both bright-field and weak-beam dark-field TEM images of a sample cross-section from sapphire to surface highlighting threading dislocations (TDs). The effective defect reduction by the in-situ SiN_x interlayer is clearly visible. Most threading dislocations (TDs) (visible as fine white lines in the weak-beam image) are stopped and only few dislocations penetrate and go on to the surface. We find no indication that new dislocations are created at the interfaces, affecting the semipolar quantum wells. Additionally, almost no

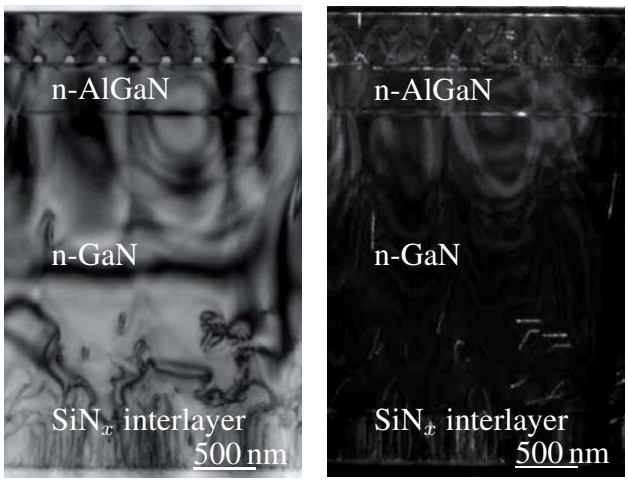

Figure 3 Bright-field (left) and weak-beam dark-field (right) TEM images. TDs (visible as fine white lines in the weak-beam image) are stopped by the in-situ SiN_x mask. The active zone is almost defect-free.

stacking faults (SFs) are found which often affect semipolar QWs.

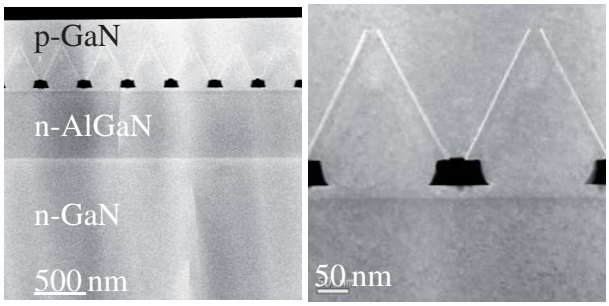

Figure 4 HAADF STEM image of the waveguide region (left). Some TDs penetrate, but almost no SFs are found. HAADF STEM image of two triangular stripes (right). The QWs show very little thickness variance along the facet.

Figure 4 shows high-angle annular dark field (HAADF) STEM images of the upper region, providing excellent Z-contrast; the AlGaN waveguide cladding is clearly visible and with very few defects present. The SiN_x mask exhibits a homogeneity of a few nanometers. A more detailed look (right) shows the homogeneity of the semipolar QW on the stripes. The thickness of the single QW stays constant and has only slight variation. The tip of the underlying GaN stripe is extremely sharp with a plateau which is a few nanometers wide.

3.2 Electro-optical characterization In order to check the optical quality of the semipolar quantum wells grown on the GaN nanostripes, samples have been grown without the Mg-doped region for temperature dependent photoluminescence. At 300 K the true green QW still shows 37 % of integrated intensity compared to 14 K, indicating a high crystalline quality and a low quantum-confined Stark effect (see Fig. 5). Figure 6 shows the

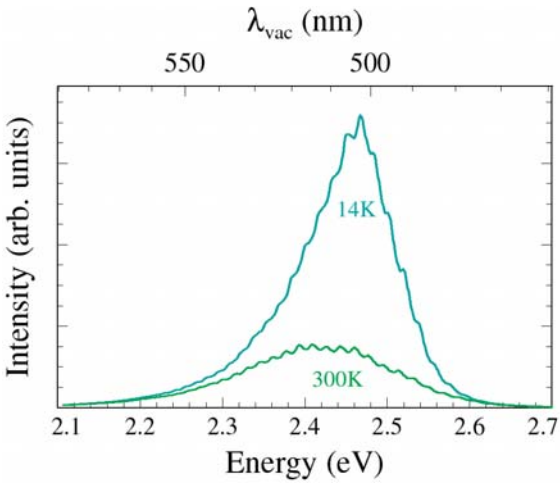

Figure 5 Temperature dependent photoluminescence spectra of true green semipolar quantum wells grown on GaN nanostripes. At room temperature, the integrated PL intensity still amounts to almost 40 % of the low temperature (14 K) value.

spectra of both blue and true green LEDs with nanostripes under 30 mA continuous excitation. The blue LEDs show a narrow spectrum with a FWHM as low as 130 meV. The true-green LED shows a considerably broader spectrum centered around 535 nm. This increased FWHM is caused by local inhomogeneities of In content and QW thickness, which lead to a blueshift for increasing current at currents below 30 mA. The spectrum is modulated by the presence of the growth mask acting as a 1D photonic crystal.

Figure 7 shows the power-current and voltage-current characteristics of both blue and true green LEDs under cw-conditions. The blue emitting LEDs have an output power higher than 1 mW at currents higher than 65 mA. The output power of the true-green LED is lower but stable over a large current range. At low current ranges, below 4 mA, no light emission is observed. As the LEDs show leakage currents at reverse operation which are comparable to planar c-oriented LEDs, measured under equivalent condi-

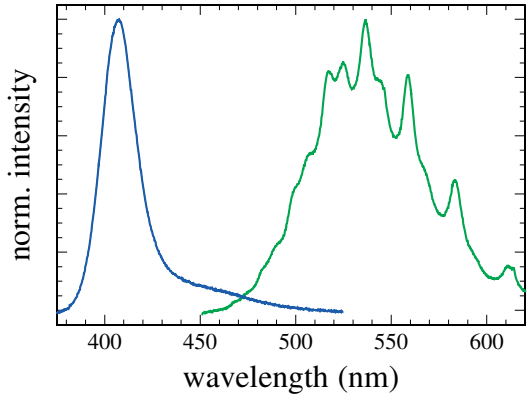

Figure 6 Electroluminescence spectra of blue and true green nanostripe LEDs with semipolar QWs.

tions (130 µA at -5.0 V), we assume that part of the recombination takes place outside the quantum wells due to the 3D p-n junction being misaligned with the quantum wells.

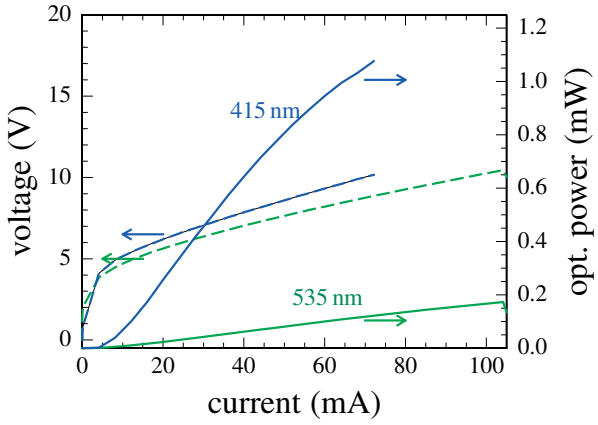

Figure 7 Optical power (solid lines) and voltage (dashed lines) characteristics of blue and true green LEDs with embedded GaN nanostripes.

4 Conclusion We have fabricated GaN based LEDs with GaN nanostripes and semipolar QWs embedded within a waveguide structure on 2-inch c-oriented sapphire substrates. Analysis by TEM and STEM shows that our nanoimprint structuring results in highly homogeneous and high quality semipolar quantum wells which are completely embedded. Electroluminescence in the blue as well as true-green wavelength region was achieved. On-wafer testing in LED operation produced electroluminescence with over 1 mW output power.

Acknowledgements Technical support from R. Rösch and R. Blood is gratefully acknowledged. Nanoimprint patterning was performed by J. Harming and C. Thanner of EVG E. Thallner GmbH. We thank S. Grözinger for TEM sample preparation. We also like to thank D. Heinz for fruitful discussions. We received financial support by the DFG within the research group FOR 957 PolarCoN.

References

[1] H. Ohta, S. P. DenBaars, and S. Nakamura, J. Opt. Soc. Am. B **27**(11), B45–B49 (2010).
[2] M. T. Hardy, D. F. Feezell, S. P. DenBaars, and S. Nakamura, Mater. Today **14**(9), 408–415 (2011).
[3] Y. Enya, Y. Yoshizumi, T. Kyono, K. Akita, M. Ueno, M. Adachi, T. Sumitomo, S. Tokuyama, T. Ikegami, K. Katayama, and T. Nakamura, Appl. Phys. Express **2**(8), 082101–1–3 (2009).
[4] M. Adachi, Y. Yoshizumi, Y. Enya, T. Kyono, T. Sumitomo, S. Tokuyama, S. Takagi, K. Sumiyoshi, N. Saga, T. Ikegami, M. Ueno, K. Katayama, and T. Nakamura, Appl. Phys. Express **3**(12), 121001–1–3 (2010).
[5] R. M. Farrell, E. C. Young, F. Wu, S. P. DenBaars, and J. S. Speck, Semicond. Sci. Technol. **27**(2), 024001–1–14 (2012).
[6] R. Kucharski, M. Zajac, R. Doradzinski, M. Rudzinski, R. Kudrawiec, and R. Dwilinski, Semicond. Sci. Technol. **27**(2), 024007–1–15 (2012).
[7] T. Sato, S. Okano, T. Goto, T. Yao, R. Seto, A. Sato, and H. Goto, Jpn. J. Appl. Phys. **52**(8S), 08JA08 (2013).
[8] F. Scholz, Semicond. Sci. Technol. **27**(2), 024002–1–15 (2012).
[9] J. Hertkorn, P. Brückner, S. B. Thapa, T. Wunderer, F. Scholz, M. Feneberg, K. Thonke, R. Sauer, M. Beer, and J. Zweck, J. Cryst. Growth **308**, 30–36 (2007).
[10] T. Wunderer, M. Feneberg, F. Lipski, J. Wang, R. A. R. Leute, S. Schwaiger, K. Thonke, A. Chuvilin, U. Kaiser, S. Metzner, F. Bertram, J. Christen, G. J. Beirne, M. Jetter, P. Michler, L. Schade, C. Vierheilig, U. T. Schwarz, A. D. Dräger, A. Hangleiter, and F. Scholz, Phys. Status Solidi B **248**(3), 549–560 (2011).
[11] B. Neubert, T. Wunderer, P. Brückner, F. Scholz, M. Feneberg, F. Lipski, M. Schirra, and K. Thonke, J. Cryst. Growth **298**, 706–709 (2007).
[12] C. Y. Cho, I. K. Park, M. K. Kwon, J. Y. Kim, S. J. Park, D. R. Jung, and K. W. Kwon, Appl. Phys. Lett. **93**(24), 241109–1–3 (2008).
[13] M. Funato, K. Hayashi, M. Ueda, Y. Kawakami, Y. Narukawa, and T. Mukai, Appl. Phys. Lett. **93**(2), – (2008).
[14] T. Wunderer, J. Wang, F. Lipski, S. Schwaiger, A. Chuvilin, U. Kaiser, S. Metzner, F. Bertram, J. Christen, S. S. Shirokov, A. E. Yunovich, and F. Scholz, Phys. Status Solidi C **7**(7-8), 2140–2143 (2010).
[15] S. Y. Bae, D. H. Kim, D. S. Lee, S. J. Lee, and J. H. Baek, Electrochem. Solid-State Lett. **15**(2), H47–H50 (2011).
[16] Y. Kato, S. Kitamura, K. Hiramatsu, and N. Sawaki, J. Cryst. Growth **144**(34), 133–140 (1994).
[17] R. A. R. Leute, D. Heinz, J. Wang, F. Lipski, T. Meisch, K. Thonke, J. Thalmair, J. Zweck, and F. Scholz, J. Cryst. Growth **370**, 101–104 (2013).
[18] D. Heinz, R. A. R. Leute, S. Kizir, Y. Li, T. Meisch, K. Thonke, and F. Scholz, Jpn. J. Appl. Phys. **52**, 062101–1–5 (2013).

[19] J. Hertkorn, F. Lipski, P. Brückner, T. Wunderer, S. B. Thapa, F. Scholz, A. Chuvilin, U. Kaiser, M. Beer, and J. Zweck, J. Cryst. Growth **310**, 4867–4870 (2008).
[20] B. Beaumont, S. Haffouz, and P. Gibart, Appl. Phys. Lett. **72**(8), 921–923 (1998).